PAPER

Optimizing dirhodium(II) tetrakiscarboxylates as chiral NMR auxiliaries†

Jens T. Mattiza,[a] Joerg G. G. Fohrer,[a] Helmut Duddeck,*[a] Michael G. Gardiner[b] and Ashraf Ghanem[c]

Thirteen enantiopure paddlewheel-shaped dirhodium(II) tetrakiscarboxylate complexes have been checked for their efficiency in the dirhodium method (differentiation of enantiomers by NMR spectroscopy); six of them are new. Their diastereomeric dispersion effects were studied and compared *via* so-called key numbers *KN*. Adducts of each complex were tested with five different test ligands representing all relevant donor properties from strong (phosphane) to very weak (ether). Only one of them, the dirhodium complex with four axial (*S*)-*N*-2,3-naphthalenedicarboxyl-*tert*-leucinate groups (**N23tL**), showed results significantly better for all ligands than the conventional complex **Rh*** [Rh(II)$_2$[(*R*)-(+)-MTPA]$_4$; MTPA = methoxytrifluoromethylphenylacetate]. On the basis of ^{1}H{^{1}H} NOE spectroscopy and X-ray diffraction, a combination of favourable anisotropic group orientation and conformational flexibility is held responsible for the high efficiency of **N23tL** in enantiodifferentiation. Both complexes, **Rh*** and **N23tL**, are recommended as chiral auxiliaries for the dirhodium experiment.
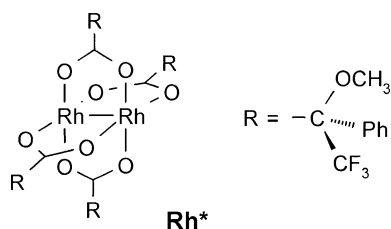
Introduction

Paddlewheel-like dirhodium tetrakiscarboxylate complexes[1] have been used in a variety of applications during the last 20–30 years; e.g, as homogenous achiral and chiral catalysts.[2] We have introduced **Rh*** (Rh(II)$_2$[(*R*)-(+)-MTPA]$_4$; MTPA = methoxytrifluoromethylphenylacetate ≡ anion of Mosher's acid; Scheme 1) as a chiral NMR auxiliary for the enantiodifferentiation of compounds with a great variety of functionalities (dirhodium method).[3] In the case of structurally related and conformationally restricted

Scheme 1 Structure of the dirhodium tetracarboxylate complex **Rh***.

[a]*Leibniz University Hannover, Institute of Organic Chemistry, Schneiderberg 1B, D-30167, Hannover, Germany. E-mail: duddeck@mbox.oci.uni-hannover.de; Fax: +49 511 7624616; Tel: +49 511 7624615*

[b]*School of Chemistry, University of Tasmania, Private Bag 75, Hobart, Tasmania, 7001*

[c]*Faculty of Applied Science, Building 3, Room D49, University of Canberra, ACT 2601, Australia*

compound families, we even found that absolute configurations can be determined by correlation.[4]

Depending on the relative molar composition, ligands form kinetically labile 1:1- or 2:1-adducts with dirhodium complexes by occupying axial positions of the dirhodium complex (Scheme 2).[5] Except for phosphanes, ligand exchange rates are generally high relative to the NMR time-scale so that time-averaged NMR signals are observed at room temperature.[3] 1:1-Adducts prevail under the standard dirhodium method conditions, *i.e.* equimolar amounts of **Rh*** and **L**, dissolved in CDCl$_3$.[3,6] Therefore, we refrain from a detailed kinetic investigation in the present study and accept this simplification for a semi-quantitative interpretation.

In the presence of a chiral dirhodium tetrakiscarboxylate complex, moderate ^{1}H and ^{13}C deshielding occur at ligand atoms close to the binding site in terms of intervening bonds.[3] This parameter, called complexation shift $\Delta\delta$ (in ppm), is an excellent indicator as to which Lewis-basic atom in the ligand binds to one of the rhodium atoms in the complex. This is particularly true for $\Delta\delta(^{13}C)$. In addition, NMR signals of chiral ligand molecules are subject to signal separation due to the formation of diastereomeric adducts. For convenience, this dispersion is designated $\Delta\nu$ (in Hz; note that $\Delta\nu$ is field-dependent); the relative intensities of the individual signals in those pairs reflect the molar ratio of the enantiomeric ligand molecules. If a ligand ^{1}H nucleus is situated above or below an aromatic ring of the MTPA residues, it is shielded, *i.e.* its signal is shifted to lower frequencies and smaller δ-values, due to the anisotropy (ring-current) effect. This effect is believed to be one of the major origins of enantiodifferentiation when using chiral auxiliaries.[7]

In an earlier study, we tried to optimise dirhodium tetrakiscarboxylates by modifying the chiral carboxylic acid residues MTPA.[8] At that time, however, our knowledge about ligand properties in
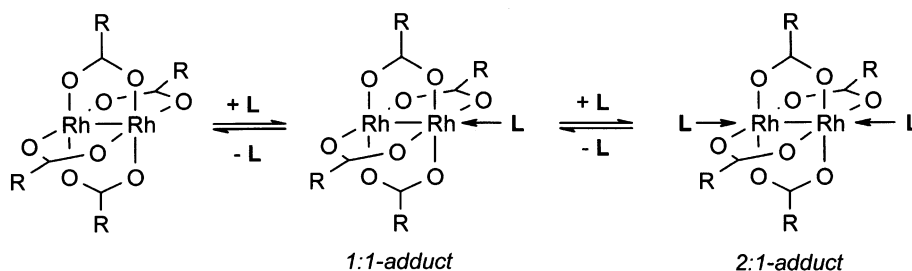
Scheme 2 Equilibria of dirhodium tetracarboxylate complexes and ligand molecules (**L**) forming 1 : 1- and 2 : 1-adducts.[5]

adduct formation equilibria was not yet developed so that success in that study was quite limited. Recently, we revisited this project by comparing the dirhodium complex **Rh*** with those containing (*S*)-2-methoxy-2-(1-naphthyl)propionate[9] and (*S*)-*N*-phthaloyl-*tert*-leucinate residues; indeed, we found trends for an improvement of dirhodium tetrakiscarboxylates as an NMR auxiliary for chiral discrimination.[10]

Results and discussion

Here we report the extension of that study in a systematic way by testing thirteen enantiopure dirhodium tetrakiscarboxylate complexes (Scheme 3). In some complexes, the carboxylate residues (equatorial ligands) are (*R*)-configured whereas others are (*S*)-configured (for details see caption of Scheme 3) depending on the availability of starting materials. However, since all five test ligands are racemic, this difference in stereochemistry does not play any role; the resulting diastereomeric adducts are mirror images of those produced by complexes with inverted absolute configurations of the carboxylates. As such, they give identical NMR data sets.

NMR methodology

The following trends towards optimizing chiral dirhodium tetrakiscarboxylate structures for enantiodifferentiation have emerged in previous studies:[8,10]

Since the diastereomeric signal dispersion $\Delta\nu$ is generated basically by anisotropy effects of aromatic groups in the carboxylates of the dirhodium complex (see above), the dispersion is expected to become larger when aromatic moieties are more extended, *e.g.* if phenyl is replaced by naphthyl. On the other hand, the size of these groups may counteract complex-ligand interaction by sterically repelling incoming ligand molecules from docking to the rhodium atoms. Therefore, it seems to be reasonable avoiding an extended aromatic group (Ar) directly attached to the α-carbon of the carboxylate (Ar-C$^\alpha$-COO). Secondly, the carboxylate should contain a further bulky group in order to reduce internal conformational flexibility since an attenuation of anisotropy effects is expected when aromatic residues are allowed to rotate about the bonds connecting them to the rest of the carboxylate. Here, however, steric congestion may again counteract by keeping attacking ligand molecules away from coming close enough to rhodium atoms.[11–15]

In order to find an optimal compromise in the design of chiral dirhodium auxiliaries, we performed standard dirhodium method experiments with a variety of dirhodium tetrakiscarboxylates

and test ligands along the following guide-lines (for the exact conditions see Experimental part):

(a) Comparing anisotropic toluenesulfonamides,

(b) Varying alkyl substituents (methyl, phenyl, benzyl and *tert*-butyl) in the carboxylates containing an anisotropic phthalimido group and

(c) Varying anisotropic imido groups (ethylene, ethenylene, phenylene, two different naphthylenes and anthrylene) in the presence of a *tert*-butyl group.

We used racemic 2-butyl derivatives as test ligands representing all categories of ligands as defined earlier[3b] (see also Scheme 3, bottom): 2-butyldiphenylphosphane (**P**) as a strong donor with a long life-time on the NMR time scale (category I), 2-butylphenylselane (**Se**; selenoether) as a strong donor with a relatively short life-time (category II), 2-butylphenylsulfane (**S**; thioether) as a moderately strong donor with an even shorter life-time (category III), 2-butylphenyloxide (**O**; ether) as a weak donor with a very short life-time (category IV). In addition, we used 2-butylacetate (**C=O**), also expected to belong to category IV).

All relevant NMR data from the various dirhodium experiments with thirteen enantiopure chiral dirhodium carboxylates and five racemic test ligands are listed in Table S1 (¹H and ¹³C chemical shifts of the ligands) and in Tables S2a to S2e (complexation shifts $\Delta\delta$ and dispersion effects $\Delta\nu$). These tables are provided in the ESI†. These data allow to identify the binding sites in the ligands, namely the hetero atoms in **P**, **Se**, **S** and **O**; in the case of **C=O** it is the carbonyl oxygen atom. Signal duplications due to diastereomeric dispersion are observed at most signals indicating binding in all classes of ligands.

For a convenient overview of the results – particularly when comparing the efficiencies of the complexes – we defined key numbers KN from the dispersion data, separately for ¹H and ¹³C, by adding the respective n_i identifiable $\Delta\nu_i$ values (in Hz, see Tables S2a – S2e in the ESI†) for a given experiment; finally the sums are divided by n_i to obtain averaged values (Table 1):

$$KN^H = [\Sigma \; \Delta\nu_i \; (^1H)]/n_i \; \{n_i\}$$
$$KN^C = [\Sigma \; \Delta\nu_i \; (^{13}C)]/n_i \; \{n_i\}$$

These averaged KN values condense the $\Delta\nu$ information of each dirhodium experiment into one single number (Table 1). They become larger when the magnitudes of individual dispersion effects ($\Delta\nu_i$) increase. As additional information, the value of n_i is given in waved brackets serving as confidence parameter; the higher n_i, the more reliable is the key number. KN numbers include very small dispersions ($\Delta\nu = 0$–1 Hz) but exclude entries where peak duplications cannot be determined safely due to signal complexity or overlap (marked by "n.d." in the Tables S2a – S2e) or by signal coalescence ("c").
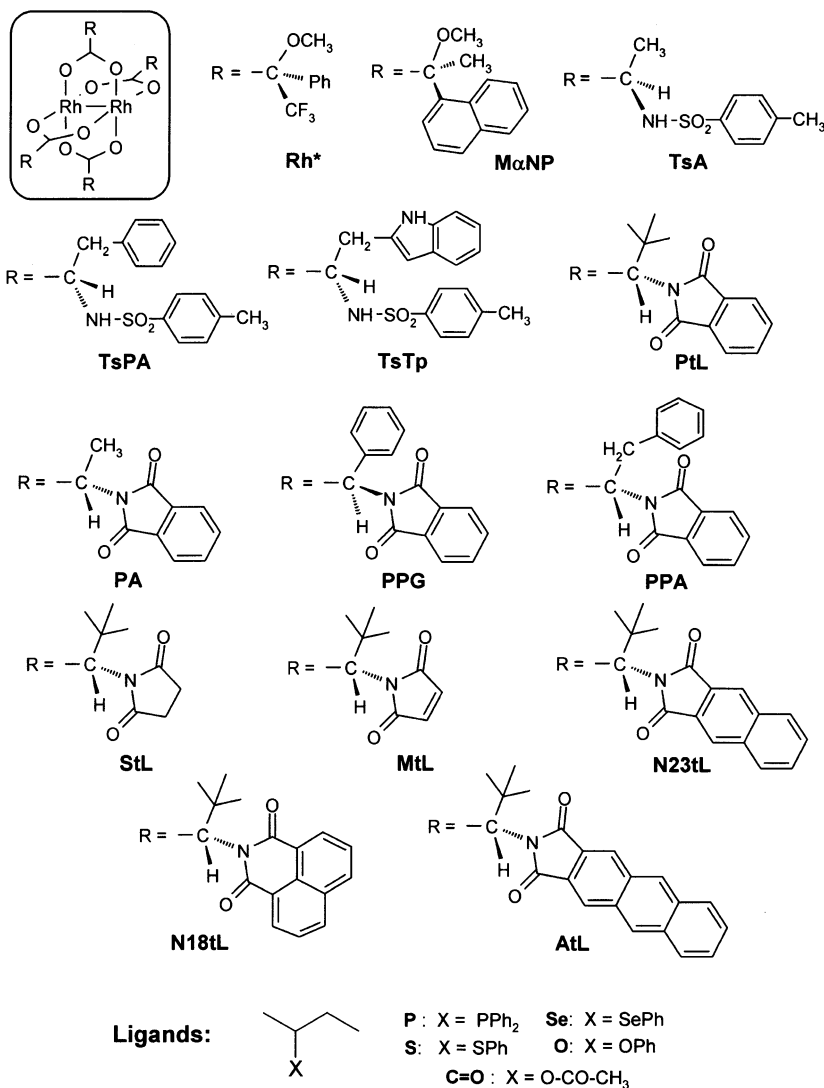
[a] Abbreviations for the dirhodium tetracarboxylates complexes were derived from the respective carboxylate residues: MαNP: (S)-2-**m**ethoxy-2-(α-**n**aphthyl)**p**ropionate; PtL: (S)-N-phthaloyl-*tert.*-leucinate; TsA: (R)-N-p-toluenesulfonylalaninate; TsPA: (S)-p-N-toluenesulfonylphenylalaninate; TsTp: (S)-3-N-(p-toluenesulfonyltryptophanate; PA: (S)-N-phthaloylalaninate; PPG: (R)-N-phthaloylphenylglycinate; StL: (S)-N-succinyl-*tert.*-leucinate; MtL: (S)-N-maleinyl-*tert.*-leucinate; N23tL: (S)-N-naphthalene-2,3-di-carboxyl-*tert.*-leucinate; N18tL: (S)-N-naphthalene-1,8-dicarboxyl-*tert.*-leucinate; AtL: (S)-N-anthracene-2,3-dicarboxyl-*tert.*-leucinate (see text); Rh*: see Introduction.

Scheme 3 Structures of the dirhodium tetracarboxylate complexes and the ligands investigated.[a]

Only the use of ^{1}H signal integrals is recommended for the determination of enantiomeric excess; ^{13}C peak areas may be obscured by NOE effects due to ^{1}H broad-band decoupling[16] although this is not very likely in diastereomeric adducts; at least, such effects have not been observed by us before.[17]

The potential of the classical **Rh*** in chiral discrimination has been elaborated in detail.[3] Therefore, the key numbers of that complex serve as standards when comparing them with those of the other twelve in order to explore their properties. *KN* values lower than corresponding ones of **Rh*** are blue in Table 1; if they are larger, they are red. In case they are larger by factor 3 or more, the numbers are bold-face. Thus, the colour pattern in Table 1 offers an easy and direct semi-quantitative overview.

(S)-2-Methoxy-2-(α-naphthyl)propionate (MαNP)

As discussed earlier,[10] **MαNP** is slightly superior to **Rh*** but failed with phosphanes at room temperature.

Toluenesulfonamides (TsA, TsPA and TsTp)

Increasing the size of anisotropic groups in the dirhodium complex may be a way to enhance dispersion effects.[10] Therefore, we started to compare the *KN* values of **Rh*** with those of three complexes containing p-toluenesulfonamide residues derived from alanine (**TsA**), phenylalanine (**TsPA**) and tryptophane (**TsTp**). The first complex, **TsA**, shows values quite similar to **Rh*** but it cannot

Table 1 Key numbers KN^H and KN^C describing the efficiency of chiral complexes in the standard dirhodium experiments of fourteen enantiopure dirhodium tertacarboxylates with five test ligands **P**, **Se**, **S**, **O** and **C=O** (for the structures see Scheme 1).[a,b,c]

		Rh*	MαNP	TsA	TsPA	TsTp	PtL	PA	PPG	StL	MtL	N23tL	N18tL	AtL
P	KN^H	8.1	c	6.6	c	c	c	11.9	c	c	0.4	51.8	70.4	c
		{8}		{8}				{8}			{8}	{8}	{8}	
	KN^C	5.5	c	2.2	c	c	c	2.0	c	c	0.3	10.7	22.0	c
		{12}		{12}				{12}			{12}	{12}	{10}	
Se	KN^H	1.2	3.3	1.1	4.5	c	22.1	5.0		9.5	8.6	19.1	c	c
		{8}	{8}	{8}	{8}		{8}	{8}		{8}	{8}	{8}		
	KN^C	1.6	8.5	5.5	6.4	c	13.6	11.8		21.3	9.0	8.5	c	c
		{8}	{8}	{6}	{8}	{7}	{7}	{8}		{8}	{8}	{8}		
S	KN^H	1.3	5.3	1.9	3.4	c	20.2	5.3	0.0	7.5	7.5	30.3	c	21.5
		{8}	{7}	{7}	{8}		{8}	{8}	{8}	{8}	{8}	{6}		{8}
	KN^C	4.6	7.1	4.8	4.3	c	20.9	9.1	1.1	13.9	6.1	14.5	c	13.4
		{8}	{8}	{8}	{8}		{8}	{8}	{8}	{8}	{8}	{8}		{8}
O	KN^H	0.0	0.6	0.0	0.0	0.0	1.5	0.1	0.0	0.0	0.0	3.8	2.3	0.0
		{8}	{8}	{8}	{8}	{8}	{8}	{8}	{8}	{8}	{8}	{8}	{8}	{8}
	KN^C	1.3	0.1	0.4	0.0	0.0	3.8	0.8	0.0	0.0	0.4	2.3	1.4	0.4
		{8}	{8}	{8}	{8}	{8}	{8}	{8}	{8}	{8}	{8}	{8}	{8}	{8}
C=O	KN^H	1.8	0.2	0.0	0.0	0.0	2.7	5.8	0.0	0.0	0.0	2.8	0.7	0.0
		{6}	{6}	{6}	{6}	{6}	{6}	{6}	{6}	{6}	{6}	{6}	{6}	{6}
	KN^C	0.3	0.5	0.0	0.0	0.0	1.7	11.4	0.3	0.3	0.0	2.2	0.3	0.7
		{6}	{6}	{6}	{6}	{5}	{6}	{5}	{6}	{6}	{6}	{6}	{6}	{6}

[a] Superscripts "H" and "C" of the KN values indicate the nucleus: ^{1}H or ^{13}C, respectively. [b] Blue/red color: smaller/larger by 0.3 or more than the corresponding value for **Rh***; values larger than threefold are highlighted (bold-face). [c] Entries marked by "c" indicate that the respective signal is broadened by coalescence effects at room temperature and cannot be interpreted in terms of dispersion.

be regarded superior. A similar statement can be made for the second one, **TsPA**; in contrast to **TsA**, this complex is unsuitable for phosphanes **P**, *i.e.* for category I ligands. Apparently, the adduct formation barrier is so high that both ^{1}H and ^{13}C signals are in the range of coalescence and any safe interpretation would require temperature increase in the experiment. In the case of the third complex, **TsTp**, coalescence effects are even more severe. So, we excluded amino acid sulfonamides from any further search for an optimized NMR auxiliary.

Varying the α side chain of the *N*-phthaloyl amino acid ligands (PtL, PA, PPG and PPA)

The situation is better for complexes with phthalimido substituents and different α-organyl groups R: **PA** (R = methyl), **PPG** (R = phenyl) and **PtL** (R = *tert*-butyl).

PtL, with R = *tert*-butyl, has been recognised before to be significantly superior to **Rh*** except for category I ligands (phosphanes) where coalescence effects disturb the interpretation.[10] Larger Δν-values have been ascribed to restricted conformational mobility inside the carboxylate moieties due to steric pressure exerted by the *tert*-butyls upon the phthalimido groups (Scheme 4). Apparently, anisotropic aromatic moieties are more or less fixed in its position towards incoming ligand molecules.[10–15] Thereby, they apply stronger shielding effects on ligand nuclei than **Rh***, the phenyl groups of which are conformationally more flexible. On the other hand, the coalescence effects at category I ligand signals may be
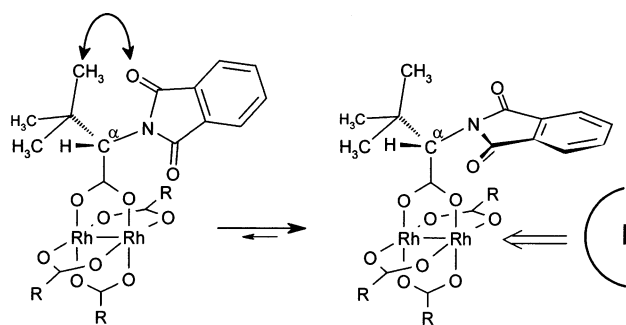
Scheme 4 Assumed preferred conformation (right) of the (*S*)-*N*-phthaloyl-leucinate residues in **PtL**; the double arrow indicates steric repulsion, **L** is the approaching ligand molecule.[10]

explained by a repulsion of the bulky 2-butyldiphenylphosphane molecules by the rigid phthalimido groups.[10]

The situation is different for **PA** with R = methyl; KN values are somewhat larger than for **Rh*** but nearly always smaller than for **PtL**. This can be rationalized satisfactorily by assuming that the methyl groups in **PA** are much less influential in steric congestion than the *tert*-butyl groups in **PtL**. In the case of the phosphane **P** a direct comparison is not possible because coalescence effects are observed when **P** interacts with **PtL**. This observation, however, is in line if one accepts that larger steric congestion leads to a hindered ligand approach (higher complex formation barrier and, hence, a higher coalescence temperature). The only exception is the

This journal is © The Royal Society of Chemistry 2011

Org. Biomol. Chem., 2011, **9**, 6542–6550 | 6545

ester ligand **C═O** which by itself is smaller and conformationally much more flexible than the other ligands so that steric effects may be overruled here by favourable molecular aggregation.

Finally, **PPG** with R = phenyl, is unqualified as NMR auxiliary for enantiodifferentiation. The internal steric congestion between the phthalimido and the phenyl groups is not clear. **PPG** does not produce any significant dispersion of ligand signals; maybe, the anisotropic effects of the two different kinds of aromatic groups counteract each other. Even worse, they produce a stronger repulsion towards ligand molecules so that the signals of both the phosphane **P** and the selenide **Se** are broadened by coalescence.

As a consequence of these comparative studies, the presence of bulky *tert*-butyl groups is recommended.

Varying the anisotropic imido groups with constant *tert*-butyl groups (PtL, StL, MtL, N18tL, N23tL and AtL)

The next question is how – in the presence of *tert*-butyl groups – the performance of **PtL** can be further improved by modifying the unsaturated moiety producing anisotropy effects. Therefore, we tested a variety of imides ranging from succinimides (**StL**) without any unsaturated carbon-carbon bond, maleimides (**MtL**) with one olefinic bond, 2,3-naphthalimides (**N23tL**) with a linearly extended aromatic system as compared to **PtL**, 1,8-naphthalimides (**N18tL**) with a lateral orientation of the aromatic system, and finally 2,3-anthrylimides (**AtL**) with the largest aromatic system of all.

StL displays some effects with strong donors except for coalescence effects of the phosphane ligand **P**, proving – to our surprise – that an aromatic moiety is not mandatory; *i.e.*, even an imido group itself can serve as a anisotropy source, although not to a satifying extent. Introducing an olefinic double bond by converting the succinimido groups in **StL** to maleinimido in **MtL** does not improve the situation; the phosphane **P** gives sharp lines but both complexes, **StL** and **MtL**, are inefficient with weak ligands. Thus, a C═C bond in addition to the imide is not of significant influence either.

The situation is completely different for **N23tL** with its linearly extended aromatic group. This auxiliary gives excellent dispersions in each of the dirhodium experiments and, as such, is superior to any of the others. This is demonstrated in Fig. 1 by a comparison of the two methyl ^{1}H signal dispersions of ligand **P** with those of **Rh***. Note the negative ^{1}H chemical shifts proving that ring-current effects are indeed operating; **PtL** is mid-way in its respective effects. Such extreme shielding has never been observed in any of our earlier dirhodium method experiments. A naphthyl group in lateral position (**N18tL**), however, diminishes the results and produces coalescence effects so that it cannot be recommended to replace **Rh*** or **N23tL** in the dirhodium experiment. Finally, the situation is even worse for **AtL** with its anthryl moiety.

As a result, **N23tL** can be regarded an optimal choice for dirhodium method experiments regardless which chiral ligands are to be investigated, although **Rh*** is sufficient in most cases.

Solution NOE experiments and dynamics of the dirhodium tetracarboxylate complexes and their adducts

Very recently, structural investigations on dirhodium complexes have been published.[11–15] It was suggested that the four ph-
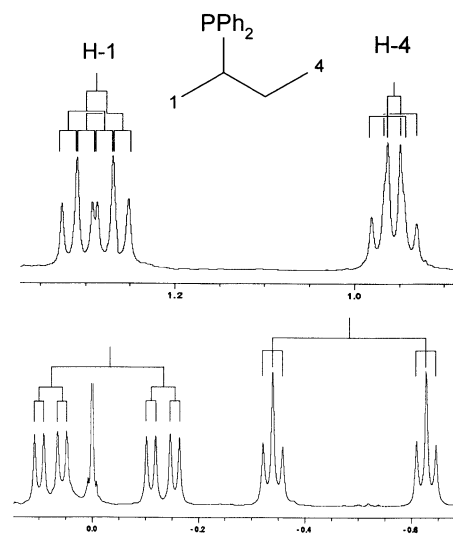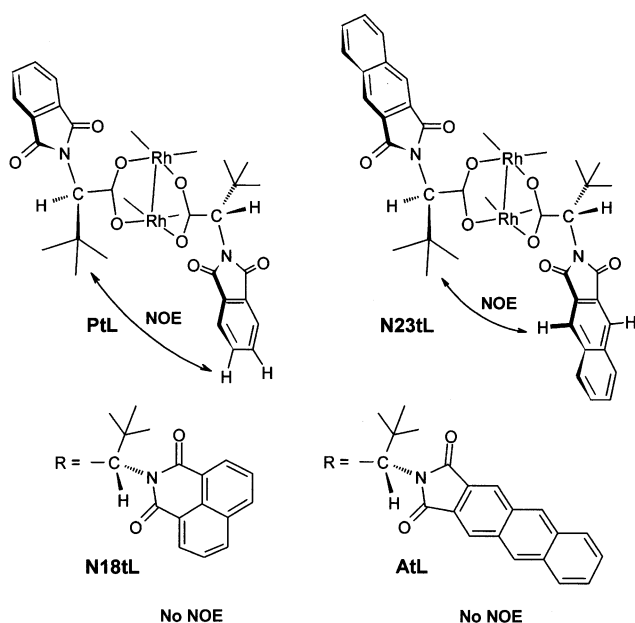

Fig. 1 H-1 and H-4 signals of the 2-butyl diphenylphosphane (**P**) (triplets, 7.5 Hz); top: in the presence of one mole equivalent **Rh***: $\Delta v = 7$ Hz (left) and $\Delta v = 6$ Hz (right), bottom: in the presence of one mole equivalent **N23tL**: $\Delta v = 86$ Hz (left) and $\Delta v = 117$ Hz (right). Note the negative ^{1}H chemical shifts in the bottom spectrum.

thalimido groups in **PtL** do not hold a stable conformation with all phthalimido groups on the same side of the dirhodium tetracarboxylate cage ($\alpha,\alpha,\alpha,\alpha$ conformation) in solution. Rather it is flexible; *i.e.*, the phthalimido groups are able to flip up and down. This was supported experimentally by heteronuclear $\{^1H\}^{13}C$ NOE experiments.[11]

The situation may be diverging in **N18L**. An X-ray diffraction experiment reveals a stable, more or less rigid complex with an $\alpha,\alpha,\alpha,\alpha$ conformation in the solid state; all four naphthalimido groups are on the same side and form a chiral, nearly squared cavity; for an analogous conformational behaviour in solution see next paragraph below.[12]

Prompted by these results, we studied the conformational behaviour of the *tert*-leucinate complexes with *N*-aromatic groups as well. Since enough hydrogen atoms are available in the aromatic parts, we performed homonuclear $\{^1H\}^1H$ NOE measurements. As shown in Scheme 5, the results are compatible with Charette's studies on **PtL**:[11] NOE responses between protons of the *tert-butyl* group and *meta*-protons in the phthaloyl can be observed arising from inter-residue contacts of those protons under the condition that at least two carboxylate residues are on different sides, up and down (α and β); distances are too far for intra-residue contacts. Analogously, we found weak NOE responses in **N23tL** (Scheme 5) indicating the presence of α,β fragments. Thus, both complexes appear to possess some flexibility. Conversely, NOE responses of that kind are absent in **N18L** and **AtL** (Scheme 5) suggesting – although not unequivocally proving! – that in solution these complexes exist, preferably at least, in the $\alpha,\alpha,\alpha,\alpha$ conformations.

These observations indicate that steric repulsion between the equatorial carboxylates and ligand molecules coming in for the axial positions (at rhodium) is an important factor in adduct formation. Apparently, a decisive criterion for an efficient chiral selector is its ability to open an easy access to the rhodium cavity, rather than extended anisotropic π electron systems. In other

6546 | *Org. Biomol. Chem.*, 2011, **9**, 6542–6550

This journal is © The Royal Society of Chemistry 2011

Scheme 5 Schematic views of some *tert*-leucinate complexes with aromatic imido groups; double arrows indicate significant NOE responses.

words, flexibility of the carboxylate residues is helpful for approaching ligand molecules to settle in the rhodium cavity.[18] This mechanism is active for **PtL** and **N23tL**, and the latter complex is a more efficient chiral selector due to its larger ring current effect. However, ligand molecules approaching **N18tL** and **AtL** with their rigid cavities encounter much stronger resistance due to the inflexibility of the cavities. Consequently, these complexes are less efficient in chiral differentiation.

X-ray crystal structure determination

X-ray crystal structure determination of the bis(methanol) adduct of **N23tL** has shown the complex to adopt an $\alpha,\alpha,\alpha,\alpha$ conformation in the solid state with all four protected *N*-substituted amino acid derived ligands being directed toward the same axial coordination of the approximately C_4 symmetric chiral paddlewheel dirhodium(II) tetracarboxylate complex. The asymmetric unit contains two molecules of this conformation; however the details of the so-called chiral crown cavities[13] of these are somewhat distinct (Fig. 2 and 3a). Molecule 1 exhibits a more regular cavity with each of the four aryl units comprising the cavity walls having a clockwise twisted arrangement. In comparison, one of the aryl units in molecule 2 has a reversed twisted arrangement that allows an edge-face π-stacking of adjacent aryl units.[13,14] Both of these cavity variants have been observed previously for related protected amino acid derived catalysts.[11,12] The potential significance of this, as well as the cavity wall steepness formed by the aryl units, has been discussed in relation to asymmetric induction in catalysis.[13–15,18] Here we simply note, again, that such minor variances are again very likely to have been influenced by solid state packing; we note that both lattice methanol and water molecules are threaded through the cavity, and *endo*-cavity face-face π-stacking of the aryl units of adjacent molecules are a solid state feature. Thus, such relatively subtle chiral cavity variants
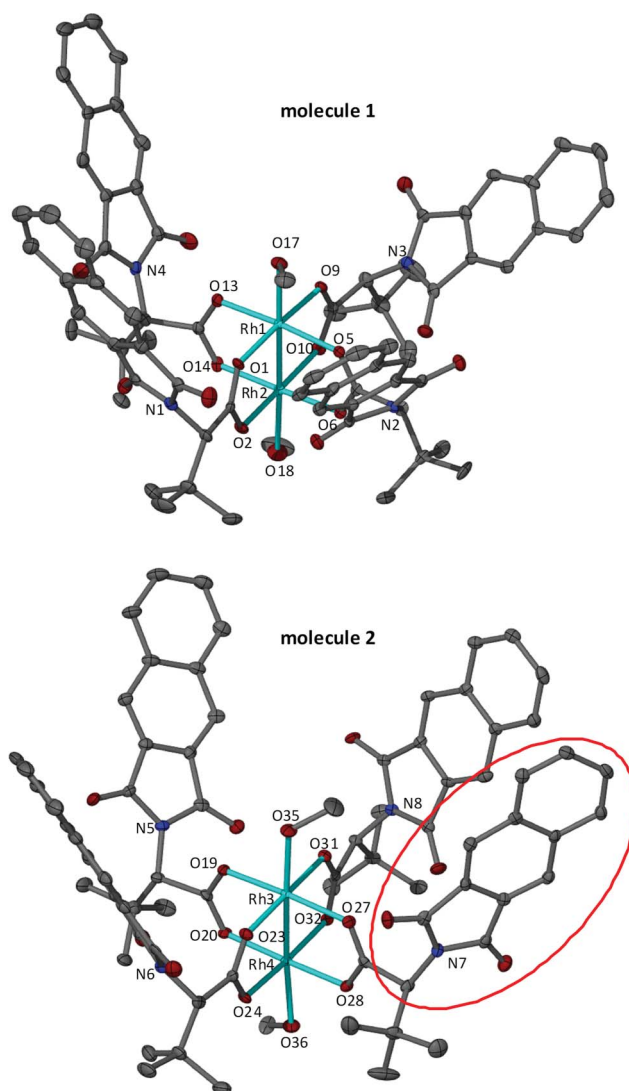
Fig. 2 Molecular structure of the bis(methanol) adduct of **N23tL**. Thermal ellipsoid diagrams have hydrogen atoms and non-Rh bound solvent molecules removed for clarity (the reverse twisted ligand of molecule 2 is circled).

may not be of great relevance to solution based reactivity but may influence the potential of the complex for chiral recognition. Clearly, through-space anisotropic interaction require less firm binding of the components than a chemical reaction.

Fig. 3b illustrates the depth of the chiral cavity that is formed from the tricyclic aryl units, reaching significantly further in the axial direction from the rhodium centre than has been recently demonstrated in other related substituted and unsubstituted *N*-phthaloyl and *N*-naphthaloyl protected amino acid-based tetracarboxylate catalysts having $\alpha,\alpha,\alpha,\alpha$ conformations.[13–15] In common with these complexes, the opposite axial coordination site of the complex is essentially achiral, being surrounded by the *tert*-butyl substituents in an approximate C_{4v} localised symmetry arrangement (Fig. 3c). Coordination of methanol at this site is clearly feasible (as indeed related complexes have featured, acetonitrile, ethyl acetate and tetrahydrofuran, for example[13–15]).
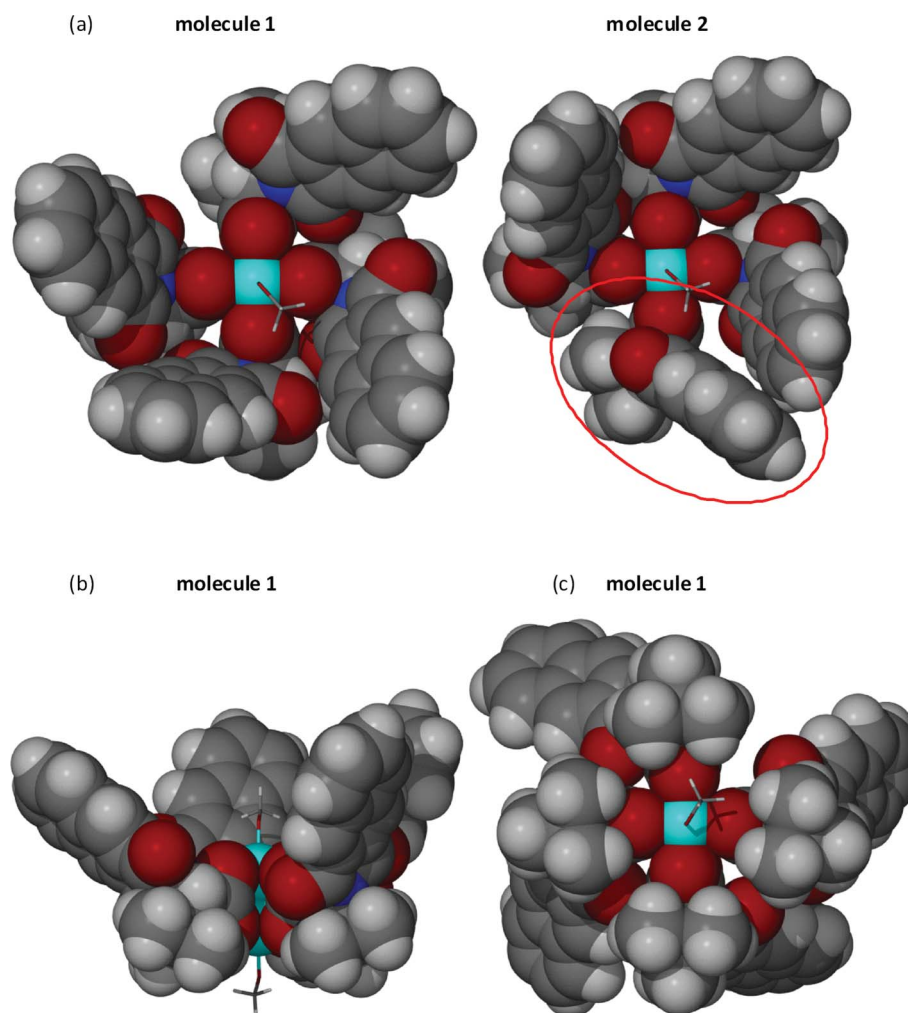
Fig. 3 Spacefilling representations of the two different bis(methanol) adducts of **N23tL** (Rh bound MeOH molecules in stick form, the reverse twisted ligand of molecule 2 is circled). (a) Molecules 1 and 2 are viewed into the chiral crown cavities down the Rh–Rh bond. (b) An equatorial O–Rh–O angle in molecule 1 is bisected to highlight the depth of the chiral crown cavity achieved with the extended chiral ligands. (c) Molecule 1 viewed from the essentially achiral *t*-Bu flanked axial coordination site [back side as compared to (a) and (b)].

With these relatively minor variants of the ligand conformations disclosed, the structures of both independent molecules in the solid state are not consistent with the solution state findings by ^{1}H NOE NMR spectroscopic studies showing correlations between the *N*-aryl and α-substituents (see above). This can be accounted for assuming that in solution the α,α,α,α conformation exists in equilibrium with other minor conformers.

Conclusion

The efficiency of thirteen dirhodium tetrakiscarboxylate complexes in the dirhodium method experiments (differentiation of enantiomers by NMR spectroscopy) has been tested and compared by studying key numbers *KN* (Table 1) representing averaged values for diastereomeric dispersion effects observed in dirhodium experiments. Five different ligands, **P**, **Se**, **S**, **O** and **C═O**, were tested for each complex, a series which represents all relevant donor categories from strong to very weak.

The structures of the aromatic ring systems and the alkyl/aryl substituents in the protected amino acids reflect a delicate balance of the dynamic conformational mobility of the complex itself influencing steric repulsion and the efficiency of anisotropy effects of aromatic moieties.

Only one of them, namely dirhodium tetrakis[*N*-2,3-naphthalenedicarboxyl-(*S*)-*tert*-leucinate] (**N23tL**), shows significantly better results for all ligands than the classical **Rh*** complex. Therefore, we recommend employing this as chiral auxiliary. Nevertheless, **Rh*** is convenient as well; dispersion effects produced by this complex are smaller but generally good enough for a reliable enantiodifferentiation *via* the integrals of ^{1}H and, eventually, ^{13}C NMR signals.

A series of ^{1}H{^{1}H} NOE experiments with the aromatic *tert*-leucinate complexes **PtL**, **N23tL**, **N18tL** and **AtL** and an X-ray diffraction study of **N23tL** suggested that it is important to account for a dynamic interplay of steric interactions between the carboxylate residues themselves as well as between these residues and approaching ligand molecules. It appears that flexible

conformations seem to be of great importance because they open a gate for the incoming ligand molecules. Among the complexes discussed here, **N23tL** constitutes the optimal compromise between conformational behaviour and anisotropy effects of the imido groups.

Experimental

NMR Spectroscopy

All ^{1}H (400.1 MHz) and ^{13}C (100.6 MHz) NMR spectra were recorded on a Bruker DPX-400 instrument (9.4 Tesla) in CDCl$_3$ with internal tetramethylsilane as standard ($\delta = 0$ ppm) for both nuclei. Digital resolutions were 0.14 Hz/point for ^{1}H and 0.24 Hz/point for ^{13}C. DEPT, HMQC and HMBC spectra (Bruker standard software) afforded safe and unambiguous signal assignments. 1D NOESY experiments[19] were performed at 500 MHz on a Bruker AVANCE 500 spectrometer using the Bruker program *selnogp* (AVANCE version 03/05/16).

In the standard dirhodium method experiment[3] the respective dirhodium tetrakiscarboxylate complex and an equimolar amount of the ligands **P**, **Se**, **S**, **C═O** or **O**, respectively, were dissolved in 0.7 ml CDCl$_3$; concentrations corresponding to ca 0.02 to 0.03 mM were prepared. Note that $\Delta\nu$-values are B$_0$-dependent; in this work all separation values are given in Hz, as determined at B$_0$ = 9.4 Tesla corresponding to 400 MHz ^{1}H and 100.6 MHz ^{13}C. Original spectra are available in the ESI.†

Syntheses

The syntheses of **Rh***,[3a] **MαNP**,[9] **PA**,[20,21] **PPG**,[22] **N18tL**,[2f] **N23tL**[2a] **N23tL** as well as the racemic ligands 2-butylphenylselenide (**Se**),[23] 2-butylphenylsulfide (**S**),[24] 2-butylphenylether (**O**)[25] and 2-butyl acetate (**C═O**)[10] and 2-butyldiphenylphosphane (**P**)[26] (Scheme 3) have been reported before. **PtL** is commercially available (TCI EUROPE N.V.). To the best of our knowledge, the complexes **TsA**, **TsPA**, **TsTp**, **StL**, **MtL** and **AtL** (Scheme 1) are new.

The complexes **TsA**, **TsPA**, **TsTp**, **PA** and **PPG** were synthesized by the same procedure as used for **Rh***.[3a] Complexes derived from *tert*-leucinates (**StL**, **MtL**, **PtL**, **N18tL**, **N23tL** and **AtLN23tL**) were prepared using a reported procedure[2d] but with a slight modification: instead of preparing the bis-methanol adduct of the commercially available dirhodium tetrakisacetate and subjecting this to the respective *tert*-leucinate in chlorobenzene, the starting material (0.15 g, 0.3 mmol) was dissolved in 0.5 ml methanol, and that solution was poured to the reaction mixture (*tert*-leucinate in chlorobenzene) after a few minutes.

Thin layer chromatography (TLC) was performed to check reaction progress using aluminum foils coated with silica gel 60 F$_{254}$ (Merck). Liquid column chromatography was performed at atmospheric pressure using silica gel 60 M, 230–400 mesh (Merck) as stationary and a mixture of petroleum ether and ethyl acetate (1 : 1) as mobile phase.

The complexes undergo decomposition on heating to 280 °C or higher so that melting points were not determined.

Although some complexes and ligands have been published before (see above), all their ^{1}H NMR, ^{13}C NMR and IR spectral data are listed in the ESI† for sake of consistency (except for **Rh*** and **MαNP**).

X-ray crystal structure determination of {Rh$_2$[(*S*)-*N*-naphthalene-2,3-dicarboxyl-*tert*-leucinate]$_4$(MeOH)$_2$} [bis(methanol) adduct of N23tL]

Small crystal size of {Rh$_2$[(*S*)-*N*-naphthalene-2,3-dicarboxyl-*tert*-leucinate]$_4$(MeOH)$_2$} [bis(methanol) adduct of **N23tL**] limited data collection to intense synchrotron X-ray radiation. Crystallization from anhydrous methanol failed to yield suitable samples and adequate results could only be obtained using bench reagent methanol of unknown water content. The subsequent structure determination described below thus established the presence of both lattice methanol and water. Crystals were found to be extremely sensitive to solvent loss and were recrystallised on site and quickly transferred to the cold stream to limit desolvation. Data was collected at −173 °C on crystals mounted on a Hampton Scientific cryoloop at the MX1 beamline ($\lambda = 0.710673$ Å) of the Australian Synchrotron.[27] The structure was solved by direct methods with SHELXS-97, refined using full-matrix least-squares routines against F^2 with SHELXL-97,[28] and visualised using X-SEED.[29] The structure exhibited minor disorder involving a Rh bound methanol solvent molecule on each of the two crystallographically independent molecules in the asymmetric unit, two lattice methanol molecules H-bonding to these as a consequence and a further lattice methanol molecule. In each case, the two site occupancy disorders were modeled with complementary occupancies of the relevant portions of the methanol molecules (in one case this necessitated the use of EXYZ/EADP cards to calculate the associated methyl protons as the molecules shared a common carbon atom). All non-hydrogen atoms were refined anisotropically except for a methyl carbon of one of the disordered rhodium bound methanol solvent molecules and an oxygen atom of a lattice water molecule. All hydrogen atoms were placed in calculated positions and refined using a riding model with fixed C–H distances of 0.95 Å (sp^{2}CH), 0.99 Å (sp^{3}CH, CH$_2$) and 0.98 Å (CH$_3$). The thermal parameters of all hydrogen atoms were estimated as $U_{iso}(H) = 1.2 U_{eq}(C)$ except for CH$_3$ where $U_{iso}(H) = 1.5 U_{eq}(C)$. The large asymmetric unit required refinement using BLOC cards. No OH protons could be located and were not calculated. A number of the above listed refinement issues have given rise to various related checkCIF alerts.

Crystal data for {Rh$_2$[(*S*)-*N*-naphthalene-2,3-dicarboxyl-*tert*-leucinate]$_4$(MeOH)$_2$} [bis(methanol) adduct of **N23tL**]: (C$_{74}$H$_{72}$N$_4$O$_{18}$Rh$_2$)$_2$·4.5(H$_2$O)·10(CH$_3$OH), M = 3458.04, orthorhombic, a = 28.965(14), b = 36.811(18), c = 15.395(16) Å, V = 16415(20) Å^3, T = 100 K, space group P2$_1$2$_1$2 (no. 18) Z = 4, 227171 reflections measured, 33748 unique (R_{int} = 0.069), 31041 > 4σ(F), R = 0.042 (observed), R_w = 0.105 (all data). CCDC 811900 contains the supplementary crystallographic data for this paper. These data can be obtained free of charge from The Cambridge Crystallographic Data Centre *via* www.ccdc.cam.ac.uk/data_request/cif.

Notes and References

1 (a) E. B. Boyar and S. D. Robinson, *Coord. Chem. Rev.*, 1983, **50**, 109; (b) *Multiple Bonds between Metal Atoms*, 2nd ed., F. A. Cotton and R. A. Walton (ed.), Clarendon, Oxford, 1993.

2 Some leading references: (a) S.-i. Hashimoto, N. Watanabe, M. Anada and S. Ikegami, *J. Synth. Org. Chem. Jpn.*, 1996, **54**, 988; (b) S. Kitagaki, M. Anada, O. Kataoka, K. Matsuno, C. Umeda, N. Watanabe and S. Hashimoto, *J. Am. Chem. Soc.*, 1999, **121**, 1417; (c) M. C. Pirrung, H. Liu and A. T. Morehead, Jr., *J. Am. Chem. Soc.*, 2002, **124**, 1014; (d) H. Tsutsui, Y. Yamaguchi, S. Kitagaki, S. Nakamura, M. Anada and S. Hashimoto, *Tetrahedron: Asymm*, 2003, **14**, 817; (e) M. Yamawaki, M. Tanaka, T. Abe, M. Anada and S. Hashimoto, *Heterocycles*, 2007, **72**, 709; (f) H. Tsutsui, N. Shimada, T. Abe, M. Anada, M. Nakajima, S. Nakamura, H. Nambu and S. Hashimoto, *Adv. Synth. Catal.*, 2007, **349**, 521; (g) A. Ghanem, F. Lacrampe and V. Schurig, *Helv. Chim. Acta*, 2005, **88**, 216; (h) M. Anada, T. Washio, Y. Watanabe, K. Takeda and S. Hashimoto, *Eur. J. Org. Chem.*, 2010, 6850.

3 (a) K. Wypchlo and H. Duddeck, *Tetrahedron: Asymm.*, 1994, **5**, 27; (b) H. Duddeck, *Chem. Rec.*, 2005, **5**, 396; (c) H. Duddeck and E. Díaz Gómez, *Chirality*, 2009, **21**, 51 and references cited therein.

4 (a) T. Gáti, G. Tóth, J. Drabowicz, S. Moeller, E. Hofer, P. L. Polavarapu and H. Duddeck, *Chirality*, 2005, **17**, S40; (b) A. G. Petrovic, P. L. Polavarapu, J. Drabowicz, Y. Zhang, O. J. McConnell and H. Duddeck, *Chem. Eur. J.*, 2005, **11**, 4257; (c) S. Moeller, Z. Drzazga, Z. Pakulski, K. M. Pietrusiewicz and H. Duddeck, *Chirality*, 2006, **18**, 395; erratum: *ibid*., p. 457; (d) E. Díaz Gómez and H. Duddeck, *Magn. Reson. Chem.*, 2009, **47**, 222.

5 Actually, rhodium atoms free of any axial ligands seem not to exist in solution; see *e.g.* F. A. Cotton, E. V. Dikarev and X. Feng, *Inorg. Chim. Acta*, 1995, **237**, 19. In the absence of intentionally added donors, solvent molecules (*e.g.* CDCl$_3$, CH$_3$OH or spurious H$_2$O) occupy these positions binding very weakly; they are replaced immediately when a stronger donor ligand **L** approaches the rhodium atoms.

6 Some proportion of 2 : 1-adducts cannot be excluded, at least if strong donor (soft) ligands are involved; see: Z. Rozwadowski, S. Malik, G. Tóth, T. Gáti and H. Duddeck, *Dalton Trans.*, 2003, 375. This, however, does not affect the present discussion.

7 T. J. Wenzel, *Discrimination of Chiral Compounds Using NMR Spectroscopy*, John Wiley & Sons, Hoboken, N.J., USA, 2007.

8 (a) C. Meyer and H. Duddeck, *Magn. Reson. Chem.*, 2000, **38**, 29; (b) C. Meyer, Fortschritte bei der Chiralen Erkennung durch ¹H-NMR- und ¹³C-NMR-Spektroskopie in Anwesenheit chiraler Dirhodiumkomplexe (Progress in Chiral Recognition by ¹H NMR and ¹³C NMR Spectroscopy in the Presence of Chiral Dirhodium Complexes), Doctoral Thesis, Leibniz University Hannover, Germany, 1999.

9 (a) N. Harada, *Chirality*, 2008, **20**, 691; (b) Y. Kasai, A. Sugio, S. Sekiguchi, S. Kuwahara, T. Tatsumoto, M. Watanabe, A. Ichikawa and N. Harada, *Eur. J. Org. Chem.*, 2007, 1811.

10 J. T. Mattiza, N. Harada, S. Kuwahara, Z. Hassan and H. Duddeck, *Chirality*, 2009, **21**, 843. This work was presented at the 20th International Symposium on Chiral Discrimination, Geneva, Switzerland, July 2008.

11 V. N. G. Lindsay, W. Lin and A. B. Charette, *J. Am. Chem. Soc.*, 2009, **131**, 16383.

12 A. Ghanem, M. G. Gardiner, R. M. Williamson and P. Müller, *Chem. Eur. J.*, 2010, **16**, 3291.

13 A. DeAngelis, O. Dmitrenko, G. P. A. Yap and J. M. Fox, *J. Am. Chem. Soc.*, 2009, **131**, 7230.

14 A. DeAngelis, D. T. Boruta, J.-B. Lubin, J. N. Plampin, III, G. P. A. Yap and J. M. Fox, *Chem. Commun.*, 2010, **46**, 4541.

15 A. DeAngelis, V. W. Shurtleff, O. Dmitrenko and J. M. Fox, *J. Am. Chem. Soc.*, 2011, **133**, 1650.

16 (a) F. W. Wehrli, A. P. Marchand and S. Wehrli, *Interpretation of Carbon-13 NMR Spectra*, 2nd ed., John Wiley & Sons, Chichester, 1988, p 405 ff; (b) J. B. Lambert and E. P. Mazzola, *Nuclear Magnetic resonance Spectroscopy – An Introduction to Principles, Applications, and Experimental Methods*, Pearson Education Inc., Upper Saddle River, NJ, 2004, p. 57.

17 Different NOE effects on ¹³C signals of corresponding nuclei in the enantiomeric ligand molecules would require significantly different longitudinal relaxation times (T$_1$) and/or a strongly diverging dynamic behaviour of the diastereomeric adducts. This, however is quite improbable.

18 E. Nadeau, D. L. Ventura, J. A. Brekan and H. M. L. Davies, *J. Org. Chem.*, 2010, **75**, 1927.

19 (a) H. Kessler, H. Oschkinat, G. Griesinger and W. Bermel, *J. Magn. Reson.*, 1986, **70**, 106; (b) J. Stonehouse, P. Adell, J. Keeler and A. J. Shaka, *J. Am. Chem. Soc.*, 1994, **116**, 6037; (c) K. Stott, J. Stonehouse, J. Keeler, T. L. Hwang and A. J. Shaka, *J. Am. Chem. Soc.*, 1995, **117**, 4199.

20 R. T. Buck, D. M. Coe, M. J. Drysdale, L. Ferris, D. Haigh, C. Moody, N. D. Pearson and J. B. Sanghera, *Tetraedron: Asymm.*, 2003, **14**, 791.

21 M. Anada and S.-i. Hashimoto, *Tetraedron Lett.*, 1998, **39**, 9063.

22 N. Pierson, C. Fernández-García and M. A. McKervey, *Tetraedron Lett.*, 1997, **38**, 4705.

23 H. Duddeck, P. Wagner and B. Rys, *Magn. Reson. Chem.*, 1993, **31**, 736.

24 J. T. Mattiza, V. J. Meyer and H. Duddeck, *Magn. Reson. Chem.*, 2010, **48**, 192.

25 E. Díaz Gómez and H. Duddeck, *Magn. Reson. Chem.*, 2008, **46**, 23.

26 (a) S. O. Grim, R. P. Molenda and J. D. Mitchell, *J. Org. Chem.*, 1980, **45**, 250; (b) M. T. Honaker, B. J. Sandefur, J. L. Hargett, A. L. McDaniel and R. N. Salvatore, *Tetraedron Lett.*, 2003, **44**, 8373.

27 T. M. McPhillips, S. E. McPhillips, H. J. Chiu, A. E. Cohen, A. M. Deacon, P. J. Ellis, E. Garman, A. Gonzalez, N. K. Sauter, R. P. Phizackerley, S. M. Soltis and P. Kuhn, *J. Synchrotron Rad.*, 2002, **9**, 401.

28 G. M. Sheldrick, *SHELX97, Programs for Crystal Structure Analysis*, Universität Göttingen, Germany, 1998.

29 L. J. Barbour, *J. Supramol. Chem.*, 2001, **1**, 189.